1-1-1980

The Electrochemical Oxidation of Substituted Catechols

Michael D. Ryan
Marquette University, michael.ryan@marquette.edu

Alice Yueh
Marquette University

Wen-Yu Chen
Marquette University

Published version. *Journal of the Electrochemical Society*, Vol. 127, No. 7 (1980): 1489-1495. DOI.

The Electrochemical Oxidation of Substituted Catechols

Michael D. Ryan,* Alice Yueh, and Wen-Yu Chen

Department of Chemistry, Marquette University, Milwaukee, Wisconsin 53233

ABSTRACT

The oxidation of substituted catechols was studied by cyclic voltammetry, chronoamperometry, rotating ring-disk electrode, and coulometry. The results showed that the quinones that were formed from the oxidation of substituted catechols reacted with the basic forms of the starting material to yield the dimeric product. These products were generally unstable and rapidly polymerized or underwent some other irreversible reaction to form an electroinactive product. For 3,4-dihydroxyacetophenone and propriophenone, the intermediate was stable long enough to be observed in cyclic voltammetry. The rate of the coupling reaction was found to correlate well with the Hammett ρ-σ parameters and indicated that there was substantial negative charge in the transition state. Finally, an analysis of the coulometric n-values along with the $i_a t^{1/2}/C$ values indicated that the initial coupling product was a diphenyl ether. Analysis of the coulometry products showed extensive polymerization.

Many workers have shown that *o*- and *p*-diphenols can be oxidized electrochemically to *o*- and *p*-quinones, respectively. The quinone that is formed is quite reactive and can be attacked by a variety of nucleophiles. Adams and co-workers (1-3) have shown that 4-methyl-*o*-benzoquinone can react with nucleophiles such as ammonia, chloride, and sulfhydryl compounds to form the addition products. In addition, Adams (4, 5) has shown that *p*-benzoquinones with electron-withdrawing substituents can be nucleophilically attacked by water to yield a trihydroxy compound, which can be further oxidized to the hydroxyquinone. Several other workers (6-9) have investigated the reactions of *o*-quinones from Dopa, catechol, and 4-methyl catechol in aqueous solutions, but the emphasis has been mostly on acidic solutions and at low concentrations, which significantly suppress the coupling reaction. Outside of the work by Stum and Suslov (10), there has been little electrochemical work done on the coupling reactions of quinones.

By contrast, there have been extensive chemical studies on the oxidative coupling reactions of phenols, and this area has been reviewed in a book by Musso (11). The ultimate products of catechol oxidations is a melanin-type product (12-14), but it is very difficult to characterize the material or to understand its coupling mechanism. There are several possible reactions which the *o*-quinone can undergo. The first possibility is the reaction of the *o*-quinone with water (reaction [1])

[1]

Because a *p*-quinone is formed when 1,2,4-trihydroxybenzene is oxidized, trihydroxybenzene is easier to oxidize than catechol. Thus, reaction [2] will occur when the trihydroxybenzene is formed

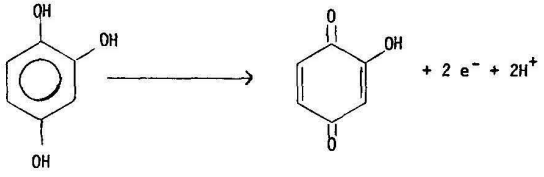

[2]

This species may then undergo a polymerization reaction (15). Alternatively, the *o*-quinone can react with the starting material, as shown in reaction [3]

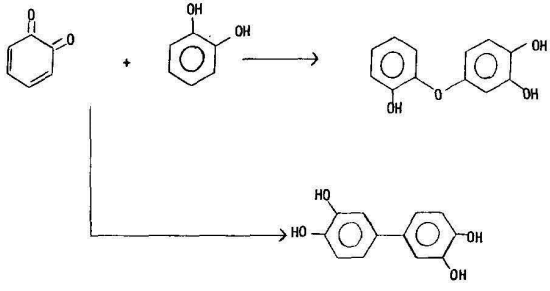

* Electrochemical Society Active Member.
Key words: cyclic voltammetry, chronoamperometry, rotating ring-disk electrode, coulometry.

Both of these products can be further oxidized to form *o*-quinones. In the above reaction, the reactive phenol may also be one of the anionic forms of catechol, which is formed by the acid dissociation reaction. Finally, the coupling reaction may occur by way of a semiquinone intermediate.

Electrochemical methods are uniquely suitable to provide information on the kinetics of the coupling reaction. The rate of disappearance of the *o*-quinone can be monitored by the use of double-step chronoamperometry or the rotating ring-disk method. The identity of new electroactive species can be monitored by cyclic voltammetry. By this approach, it is possible to understand the initial steps that are involved in the coupling reaction.

Experimental

Equipment.—Most of the electrochemical experiments were performed on a homemade three-electrode potentiostat of conventional design. Some of the cyclic voltammetric experiments were done on a Princeton Applied Research Corporation (PAR) Model 174A polarographic analyzer. The reference electrode was a saturated calomel electrode (SCE) and the working electrode was a carbon paste electrode. A platinum wire was used as an auxiliary electrode. The chronoamperometric and cyclic voltammetric data were recorded on a Hewlett-Packard 7045A X-Y recorder or a Tektronix Model D15 storage oscilloscope. The u.v.-visible spectra were recorded on a Cary 14 spectrometer. The coulometry was performed on a PAR Model 173 potentiostat with a Model 179 integrator. The ring-disk electrode rotator was a Pine Instrument Company Model ASR, the ring and disk were platinum, and a homemade bipotentiostat was used as described in Ref. (16).

Catechol (CAT), 3,4-dihydroxacetophenone (DHAP), 3-methyl catechol (3MC), 4-methyl catechol (4MC), 3,4-dihydroxybenzoic acid (DHBA), and 3,4-dihydroxyphenylacetic acid (DHPA) were purchased from Aldrich Chemical Company. 3,4-Dihydroxypropriophenone (DHPP) was obtained from ICN Pharmaceutical Incorporated. 3,4-Dihydroxybenzoic acid, ethyl ester (DHBE) was obtained from Pfaltz and Bauer, Incorporated. Catechol and 3-methyl catechol were purified by sublimation. DHBE was recrystallized from hot water, and pale yellow crystals were obtained with a melting point of 198°-200°C. 3,3',4,4'-Tetramethoxy biphenyl (TMBP) was synthesized by the Ullmann reaction, as described in Ref. (17), and the TMBP was reacted with boron tribromide (18) to yield the 3,3',4,4'-tetrahydroxybiphenyl (THBP).

All solutions were prepared from deionized water. The *p*H 1 solutions were made with sulfuric acid. The solutions that were buffered around *p*H 5 were made from acetic acid/acetate mixtures, while phosphate buffers were used for solutions above *p*H 6.

Results

Cyclic voltammetry.—Only one oxidation peak was observed for all the catechols studied except for THBP, DHAP, and DHPP. With the same exceptions, only one reduction peak was seen, except in basic solutions where the quinone was unstable. In that case, the reduction peak disappeared. The quasi-reversibility of the electron transfer reaction makes it difficult to obtain quantitative kinetic data from the cyclic voltammograms but one can see qualitatively that the quinone becomes progressively less stable as the *p*H is raised. The effect of *p*H on the cyclic voltammetry of catechol is shown in Fig. 1. In addition. the second-order nature of the reaction process can be seen by the decrease in the peak current ratio, i_{pc}/i_{pa}, as the concentration is increased at a given *p*H and scan rate. A quantitative measurement of this effect is described later in this work.

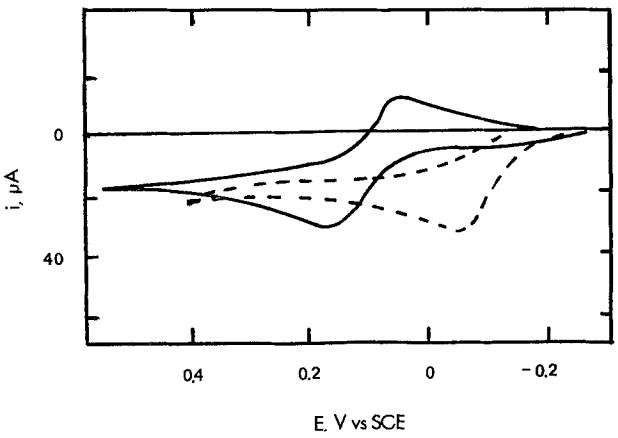

Fig. 1. Cyclic voltammetry of 0.3 mM catechol. Solid line *p*H 2. Dashed line *p*H 8. Scan rate 10 mV/sec.

The oxidation of DHAP and DHPP gives additional features that are instructive in understanding the reaction process. In solutions with a *p*H less than 5, the cyclic voltammetry of these two compounds is similar to the other catechols. But, for *p*H values between 5 and 7, a new redox couple is seen in the voltammograms, as shown in Fig. 2. For DHPP, the new oxidation wave is not seen until the second scan because its peak potential is less than the peak potential for catechol, while the new oxidation peak for DHAP is more positive than the catechol peak and hence is seen in the first scan. In Fig. 2, curve C, one can see that this new peak is reduced relative to the first peak as the scan rate is increased. At first glance, this behavior looks similar to the behavior seen for 2,5-dihydroxyacetophenone (4), where water adds to

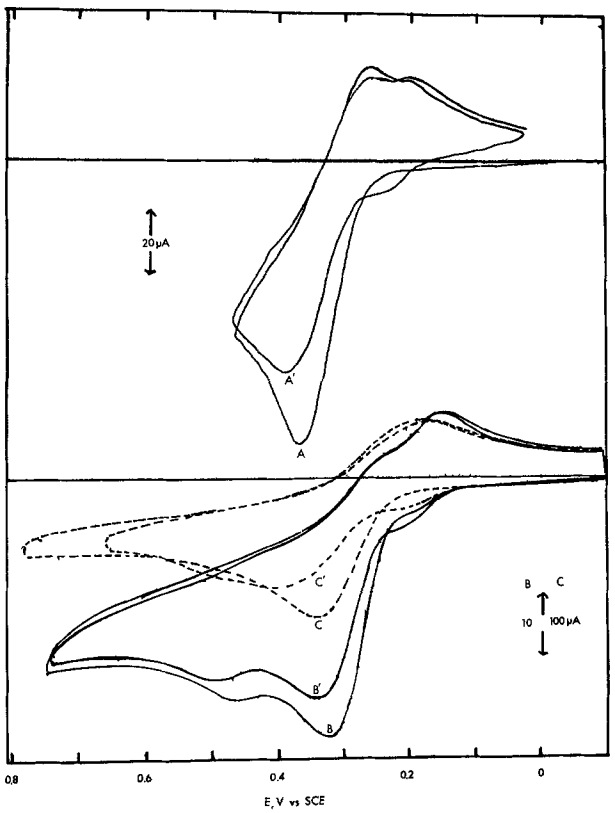

Fig. 2. A (first scan) and A' (second scan): cyclic voltammetry of 1.0 mM dihydroxypropiophenone, *p*H = 5.8; scan rate 30 mV/sec. B (first scan) and B' (second scan): cyclic voltammetry of 1.0 mM dihydroxyacetophenone (DHAP), *p*H = 6.0; scan rate 10 mV/sec. C (first scan) and C' (second scan): cyclic voltammetry of 1.0 mM DHAP; *p*H = 6.0; scan rate 100 mV/sec. Solid lines are the zero current for each voltammogram.

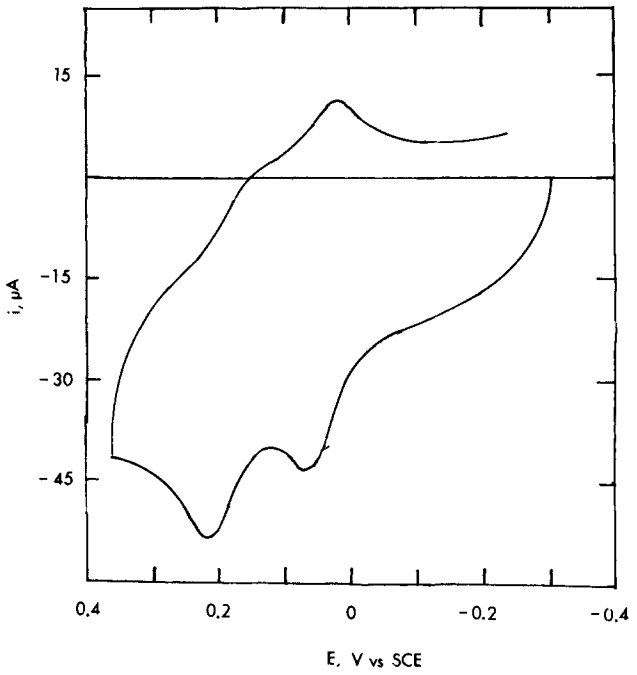

Fig. 3. Cyclic voltammetry of 0.1 mM 3,3', 4,4'-tetrahydroxybiphenyl; pH 7.0; scan rate 100 mV/sec.

the quinone. But, on quantitative examination, the peak current function, $i_{pa}/v^{1/2}C$, does not increase but remains constant at the value for two electrons. This will be examined in more detail later by chronoamperometry. In more basic solutions, both reduction waves and the new oxidation wave disappear.

The oxidation of THBP is shown in Fig. 3. Two oxidation waves occur, and on the basis of previous work, the following scheme can be proposed

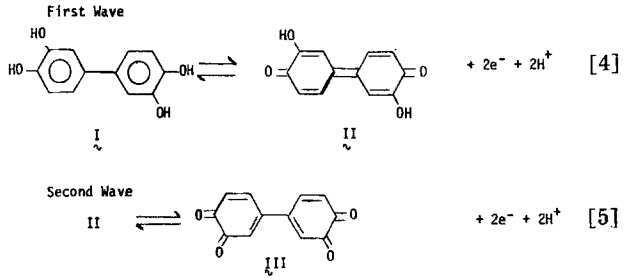

The peak potential of the second wave is approximately at the same potential as the peak potential of catechol at the same pH. It should be noted that, except for catechol and 3-methyl catechol, none of the other biphenyls formed from their respective catechols can form structure II because of the repulsion of the 4-substituents on the rings. As a result, it is impossible for the biphenyl to form the planar configuration needed for the extended p-quinone structure.

Chronoamperometry.—In order to calculate the rate of reaction of the electrochemically generated quinone, double-potential step chronoamperometry (DPS) was used to eliminate the effect of the electron transfer rate. The chronoamperometric behavior of catechol was typical of all the substituted catechols where no new peaks were observed in the cyclic voltammograms. The current decay of the oxidation current for catechol obeyed the Cotrell equation for all the pH values studied ($1 < pH < 12$). The value of the current constant, $i_a t^{1/2}/C$, was equal to the value expected for a two-electron oxidation, even for times when there was substantial reaction of the quinone. The current ratio i_c/i_a, was dependent on the step time, τ, the concentration of catechol, and the pH. The first two

Table I. The chronoamperametric data for catechol at pH 8

Conc (mM)	Time (sec)	i (μA)	$i_a t^{1/2}/C$	i_c/i_a	R_I
0.30	0.50	97.5	230	0.275	0.951
	1.0	67.8	209	0.262	0.904
	2.0	46.9	221	0.264	0.912
	5.0	29.4	219	0.260	0.875
	10.0	20.8	219	0.223	0.769
1.00	1.0	209	207	0.274	0.943
	2.0	148	209	0.256	0.882
	5.0	93.6	207	0.199	0.688
	10	66.6	210	0.135	0.466
	15	54.1	209	0.123	0.425
	20	47.2	211	0.083	0.288
3.00	0.5	1087	256	0.268	0.926
	1.0	679	226	0.228	0.786
	2.0	454	214	0.221	0.762
	5.0	278	222	0.131	0.450
	10	210	221	0.073	0.250
	15	171	220	0.048	0.165
	20	148	221	0.037	0.127

effects can be seen in Table I for three different concentrations of catechol at pH 8. In all cases, the current ratios are divided by 0.2928 to normalize the values. This new parameter is called R_I. These data demonstrate the second-order nature of the reaction process. The current ratio data from Table I can be correlated with the theoretical working curve for the following coupling mechanism

$$A \rightleftharpoons B + 2e^- + 2H^+ \qquad [6]$$

$$B + A \xrightarrow{k_d} D \qquad [7a]$$

$$D \rightarrow D' + 2e^- + 2H^+ \qquad [8]$$

$$D + B \rightleftharpoons A + D' \qquad [9]$$

It is assumed that reaction [8] is irreversible because no new wave is seen for the D/D' couple. Since reaction [8] is favorable, reaction [9] must also be occurring and may very well be the most probable means of forming D'. The current ratio data from Table I is shown in Fig. 4, along with the theoretical lines. It should be pointed out that an alternate coupling scheme could be

$$2B \xrightarrow{k'_d} D' \qquad [7b]$$

The chronoamperometric working curve for R_I as a function of τ is somewhat different for this case, but the difference is not large. As will be seen later, though, the pH variation of the rate constant is more consistent with reaction [7a].

The variation of the coupling rate constant, k_{obs}, with pH is shown in Table II, along with the $i_a t^{1/2}/C$ values. This variation was consistent with the following coupling mechanism

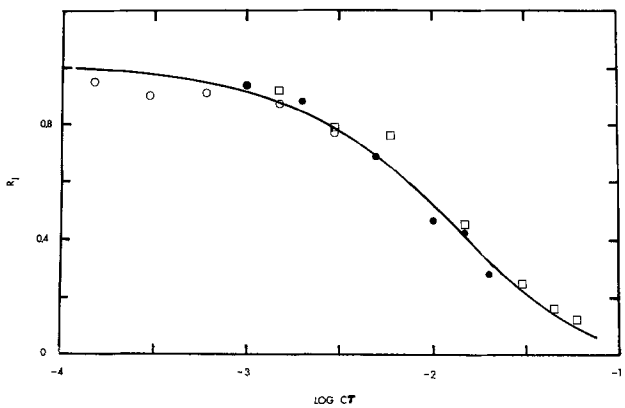

Fig. 4. Chronoamperometry of catechol at pH 8. Concentration of catechol: (○) 0.30 mM, (●) 1.00 mM, and (□) 3.00 mM. Line is theoretical line for a second-order coupling mechanism with a rate constant of 30 $M^{-1}sec^{-1}$.

Table II. Variation of the rate of the coupling reaction as a function of pH

pH	k_{obs} (M^{-1} sec^{-1})	α_1*	k_1 (M^{-1} sec^{-1})	α_2*	k_2 (M^{-1} sec^{-1})	k_{calc}† (M^{-1} sec^{-1})
8.0	30	0.059	507	1.18×10^{-5}	—	29
9.0	158	0.387	410	7.71×10^{-4}	—	188
10.0	456	0.848	537	1.69×10^{-2}	—	411
11.0	1398	0.823	802	0.164	4500	754
12.0	1610	0.333	(485)‡	0.666	2175	1605

* $pK_1 = 9.2$, $pK_2 = 11.70$, Ref. (20).
† Calculated value of k_{obs} from the best fit of the data.
‡ Calculated from the pH 8-11 data.

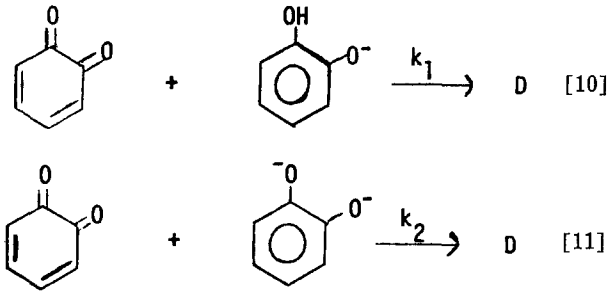

The value of k_{obs} is then

$$k_{obs} = \alpha_1 k_1 + \alpha_2 k_2 \quad [12]$$

where α_1 and α_2 are the fraction of the catechol in the first and second ionized forms, respectively, as defined in Eq. [13] and [14]

$$\alpha_1 = K_1[H^+]/([H^+]^2 + K_1[H^+] + K_1K_2) \quad [13]$$

$$\alpha_2 = K_1K_2/([H^+]^2 + K_1[H^+] + K_1K_2) \quad [14]$$

where K_1 and K_2 are the first and second acid dissociation constants, respectively. If k_2 is not much larger than k_1, then, when the pH < pK_2, $\alpha_2 k_2$ is negligible compared to $\alpha_1 k_1$, as a result, k_1 is then

$$k_1 \approx k_{obs}/\alpha_1$$

The calculated values of k_1 are shown in Table II, along with the k_2 values calculated from the best values of k_1 and Eq. [12]. In Table II, the best values for k_1 and k_2 are used with Eq. [12] to calculate the value of k_{obs} at each pH, and this will be called k_{calc}. The values of k_{obs} as a function of pH are shown in Fig. 5 along with the theoretical line based on the known α values and the measured rate constants.

This same procedure can be used to calculate the values of k_1 and k_2 for other catechols, except for DHPP and DHAP. The values of k_{obs} are small enough so that k_1 and k_2 can be calculated for 3MC, 4MC, and DHPA. The coupling reaction is too fast to measure the values of k_{obs} in very basic solutions which are necessary to calculate k_2 for DHBA, DHAP, DHPP, and DHBE. The variation of k_{obs} as a function of pH for these compounds are shown in Fig. 5 and 6. The values of k_1 and k_2 are given in Table III for all the catechols studied, along with the literature values for pK_1 and pK_2.

Table III. Values of k_1 and k_2 for substituted catechols

Compound	k_1 (M^{-1} sec^{-1})	k_2 (M^{-1} sec^{-1})	pK_1	pK_2
CAT	485	2170	9.2	11.7
3MC	82	580	9.3	11.8
4MC	440	660	9.5	11.9
DHPA	140	1500	10.0	11.6
DHBA	4,900	—	10.2	—
DHAP	60,000	—	8.20	—
DHBE	1,800	—	8.08	11.65
DHPP	66,000	—	8.20	—

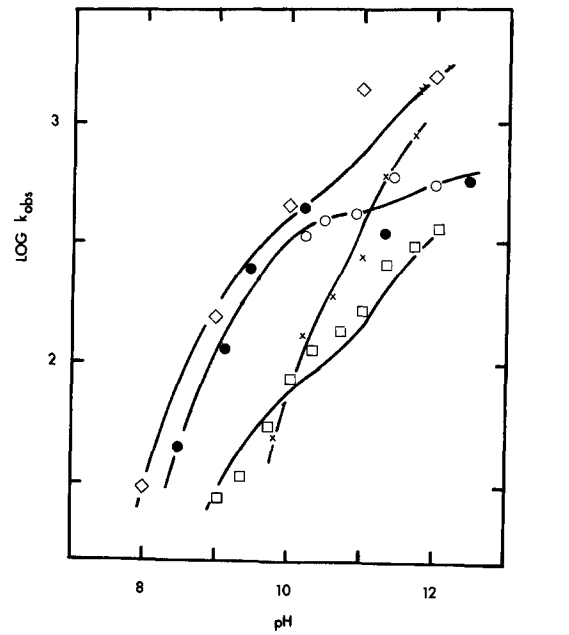

Fig. 5. Variation of the observed rate constant, k_{obs}, as function of pH. (◇) catechol, (□) 3-methyl catechol, (●) 4-methyl catechol using chronoamperometry, (○) 4-methyl catechol using rotating ring-disk method, (×) dihydroxyphenylacetic acid. Solid lines are the theoretical curves using Eq. [12].

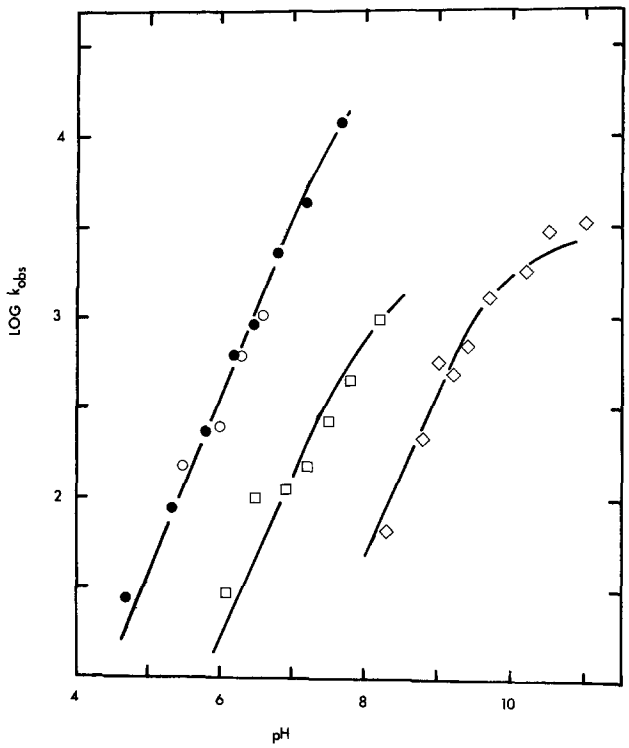

Fig. 6. Variation of the observed rate constant k_{obs}, as a function of pH. (●) dihydroxypropiophenone, (○) dihydroxyacetophenone, (□) dihydroxybenzoic acid, ethyl ester; (◇) dihydroxybenzoic acid. Solid lines are the theoretical curves using Eq. [12].

The measurement of k_{obs} for DHAP and DHPP must take into account the electroactivity of the reaction product. The working curve for an electroactive D/D' couple was derived by the use of the finite-difference approach (19). The following reaction mechanism was numerically solved

$$A \rightleftharpoons B + 2e^- + 2H^+ \quad [6]$$

$$B + A \xrightarrow{k_d} D \quad [7a]$$

$$D \rightleftharpoons D' + 2e^- + 2H^+ \quad [15]$$

$$D + B \rightleftharpoons A + D' \quad [9]$$

$$D' + A \xrightarrow{k_t} T \quad [16]$$

$$T \rightarrow T' + 2e^- + 2H^+ \quad [17]$$

where T and T' are the reduced and oxidized forms of the trimer, respectively, and k_t is the rate of the trimer reaction. Qualitatively we can see from cyclic voltammetry that the stability of the dimer peak depends on the concentration of the catechol. The working curve for this mechanism for different ratios of k_d/k_t is shown in Fig. 7.

The analysis of the DHPP data is illustrated in Fig. 8 for the chronoamperometric data at pH 6.8 for three different concentrations. For $R_I > 0.5$, the value of k_{obs} depends mostly on the dimerization rate while the value of k_t can be calculated most accurately for R_I values less 0.5. From this information, it was found that k_d was $1.0 \times 10^3\ M^{-1}\ sec^{-1}$ and k_t was $1.0 \times 10^2\ M^{-1}\ sec^{-1}$. One must remember that both k_d and k_t depend on pH and are observed rates that depend on α_1 and α_2. Data for different pH values are shown in Fig. 9, and the variation of k_d with pH is shown in Fig. 6. From this, k_1 was found to be $6.6 \times 10^4\ M^{-1}\ sec^{-1}$ and $k_{1,t}$ or k_1 for the trimer reaction was $1.3 \times 10^4\ M^{-1}\ sec^{-1}$. Similar data were obtained for DHAP. The potential for the anodic step was always chosen positive of the second peak. It is interesting to note that the value of $i_a t^{1/2}/C$ remained at the value indicative of two electrons even when there was substantial reaction for the quinone.

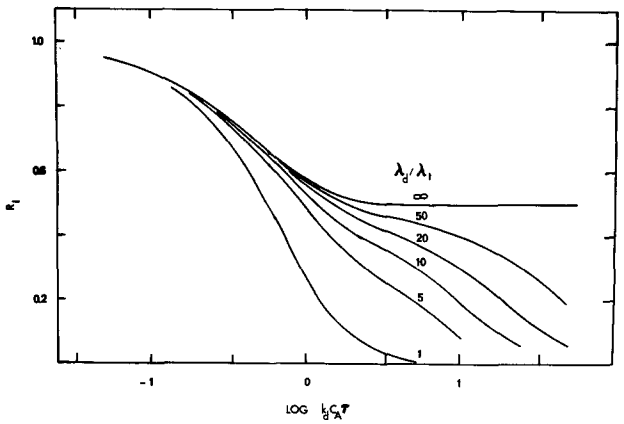

Fig. 7. Theoretical working curve for a dimer-trimer coupling reaction. $\lambda = k_d C\tau$, where k_d is the rate of dimerization reaction. $\lambda_t = k_t C\tau$, where k_t is the rate of the trimerization reaction.

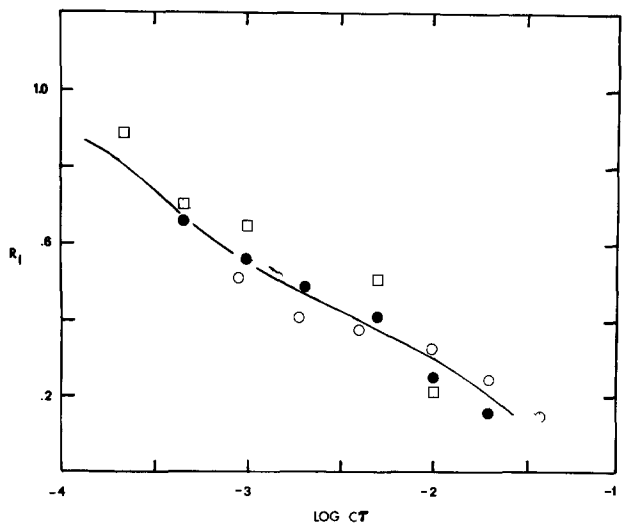

Fig. 8. Double potential step chronoamperometry of dihydroxypropiophenone at pH 6.8. Concentration of DHPP: (□) 0.5 mM, (●) 1.0 mM, (○) 2.0 mM.

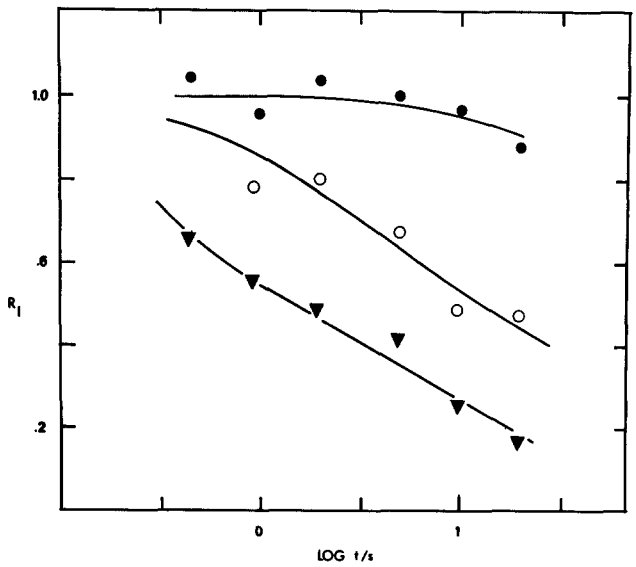

Fig. 9. Double potential step chronoamperometry of 1.0 mM dihydroxyprophenone. (●) pH = 5.8, (○) pH = 6.2, (▼) pH = 6.8.

Rotating ring-disk experiments (RRDE).—4MC was studied by RRDE in order to verify that surface filming or other such effects were not occurring. The appearance of steady-state currents (especially for the ring) and the obtaining of kinetic data consistent with the chronoamperometry were a further verification that the homogeneous reactions were being monitored.

Only one oxidation wave was observed on the disk as the disk potential was scanned (Fig. 10). If the ring potential was held at a potential where the quinone is reduced, a reduction wave was seen as the disk potential was scanned through the oxidation wave (Fig. 10). In addition, if the disk potential was held in the limit-

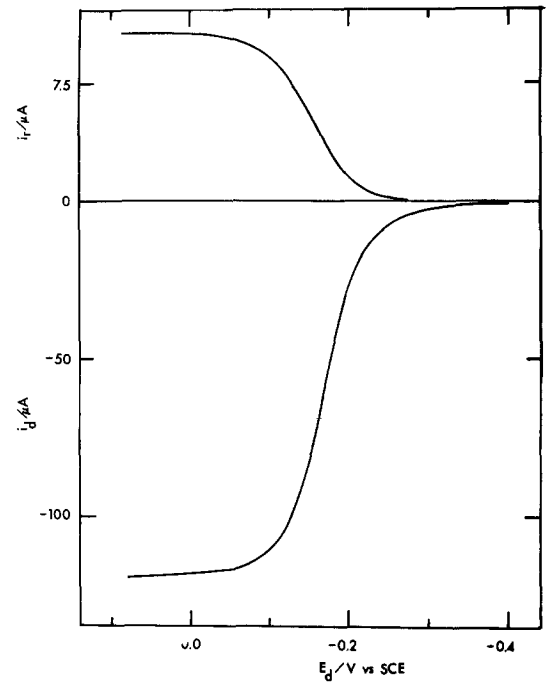

Fig. 10. Rotating ring-disk voltammogram of 0.93 mM 4-methyl catechol. i_r = ring current. i_d = disk current. pH = 12. ω = 10.5 sec^{-1}.

ing current region and the ring potential was scanned, only one wave corresponding to the quinone reduction was observed. For all pH values studied, the disk limiting current, i_D, was proportional to the square root of the rotation rate, $\omega^{1/2}$. For $n = 2$, the diffusion coefficient, D, for 4MC was calculated to be 4.64×10^{-6} cm²/sec.

In acidic solutions, the collection efficiency, N_k, was independent of the rotation rate, ω, and was equal to 0.17, which was the maximum collection efficiency. In neutral and basic solutions, the collection efficiency decreased and was dependent on rotation rate. A typical set of data is shown in Fig. 11, along with the theoretical curve for the coupling mechanism. The second-order rate constant was calculated for different pH values and the results are shown in Fig. 5. These results were quite consistent with chronoamperometry.

Coulometry.—The coulometric oxidation of 4-methyl catechol was studied most extensively with less work being done on catechol, DHBA, and DHPP. All of these compounds gave similar results. The oxidation of these compounds leads to extensive polymerization as has been seen by previous workers (11). In particular, in this work the products of the oxidation of DHBA and DHPP were isolated and were found by mass spectrometry to be highly polymerized. Fragments were seen in the mass spectra for monomers, dimers, and trimers and the high melting point (>200°C) indicated even larger polymers. This is consistent with the chronoamperometric work which showed the poor stability of the dimer.

The current decay curve for the oxidation of 4MC depended somewhat on pH. In very basic solutions such as pH 11.2, the coulometric n-value was 2.12 which is consistent with the voltammetric and chronoamperometric data. An analysis of the log i-t curve at this pH also gave a slope with an n-value of 2.07. In less basic solutions, the log i-t curve tended to flatten out at long times and the overall coulometric n-value rose to 3.03 at pH 9.42. Still, for the first 10-15 min of the electrolysis, the slope of the log i-t curve yielded a value of 2.05. This indicated that in less basic conditions and at longer times an electroactive product was slowly being formed. This is at much too long a time scale to be observed in chronoamperometry or voltammetry and is probably related to the polymerization reaction. During the time scale for the chronoamperometric work, though, an overall $n = 2$ process occurred. Similar results were observed for DHBA where an n-value for the log i-t curve was initially 2.13 while the overall n-value was 2.91 at pH 10.62. Once again, the increased n-value was due to some slowly formed electroactive product which occurred during further polymerization.

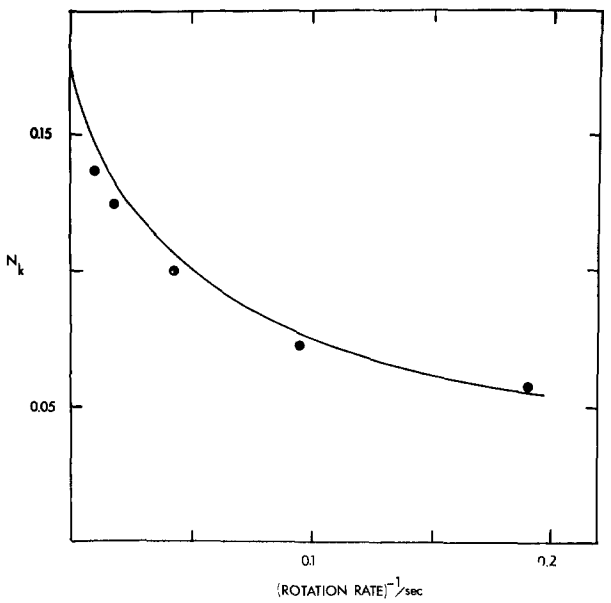

Fig. 11. Variation of the collection efficiency, N_k, as a function of the reciprocal of rotation rate for 0.93 mM 4-methyl catechol. pH = 12. Points are experimental points and solid line is the theoretical curve for $k_f = 620$ M^{-1} sec^{-1}.

Discussion

The oxidation of all the catechols studied involved initially the oxidation of the catechol to the o-quinone

[18]

The next step was the coupling between the starting material, catechol, and the quinone

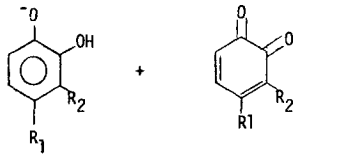

[19]

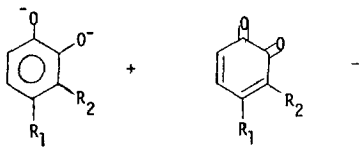

[20]

The identity of D can only be inferred because of its poor stability and the great tendency of the quinones to polymerize. Two general types of D, which are formed by C-O or C-C coupling, can be visualized

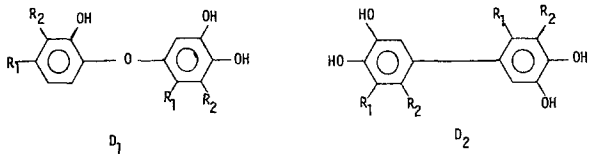

There are also several other isomers that can be formed by coupling at other positions. Dimer D_1 can be further oxidized as shown in reaction [21]

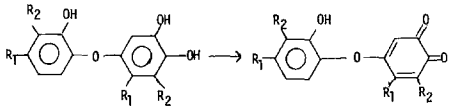

[21]

and D_2 can be oxidized as follows

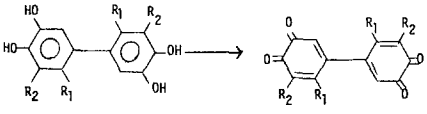

[22]

There is an intermediate two-electron oxidation state for these catechols such as D_2' for catechol (R_2 = H) or 3-methyl catechol ($R_2 = CH_3$) or D_2'' for the other catechols

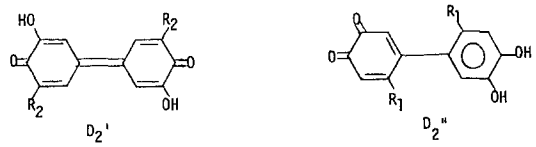

Since D_2 can be oxidized by four electrons at the potential that the oxidation occurred the overall oxidation of catechol by the C-C coupling is given in reaction [23]

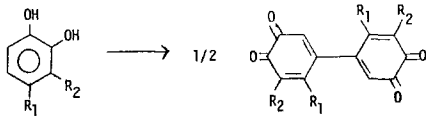

[23]

Conversely, the overall oxidation of catechol to D_1' is

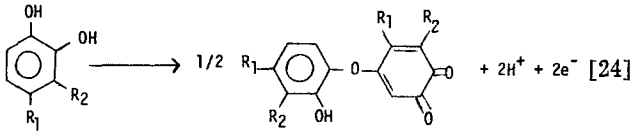

Thus, if reaction [23] were occurring, the $i_a t^{1/2}/C$ values should increase by 50% when the coupling reaction occurs to a significant extent. But if reaction [24] were occurring, the $i_a t^{1/2}/C$ values should remain constant, as was observed. In addition, the coulometric n-values were consistent with an $n = 2$ oxidation process. It is only when the coupling process is slow (low pH) and when the catechol concentration is depleted (long electrolysis time) that the coulometric n-value increases. In those cases, extensive polymerization is occurring and the decreases in the catechol may cause changes in the polymerization mechanism. In general, though, the formation of dimer D_1 is the most probable step in initiating the polymerization process for catechol. The electroinactivity of the product is probably due to the rapid polymerization or some yet uncharacterized irreversible reaction. Dimer D_2 has been shown in this work to be electroactive and, in all probability, dimer D_1 should also be electroactive. It is only for DHAP and DHPP that the reaction of the dimer is slow enough to be observed in voltammetry.

The coupling reaction is quite sensitive to substituent effects as was seen in Table III. The rate of the coupling reaction, k_1, can be related with the Hammett ρ-σ parameters, where the Hammett equation is

$$\log k_i = \log k_o + \rho\sigma$$

where k_i is the rate constant for the substituted catechol, k_o is the rate constant for catechol, σ is a constant characteristic of a given substituent group, and ρ is the slope of the log k_i-σ graph. The Hammett plot is shown in Fig. 12. The ρ value was 6.2. This positive ρ value means that the transition state has a substantial negative charge because the reaction rate is increased significantly for electron-attracting substituents. This result is consistent with the attack of the catechol anion on the quinone. The only exception is the coupling of DHBE, which deviates significantly from the log k_i-σ line. This deviation may be due to steric effects.

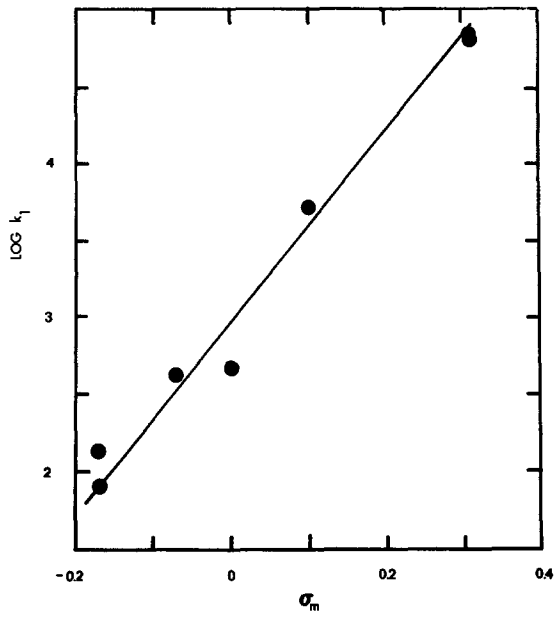

Fig. 12. Hammett σ-ρ plot for the catechols studied

The best fit was obtained for σ_m values, although σ_p gave similar results but with somewhat more scatter. This may be a reflection of the point of attack by the anion, although it is difficult to make any firm conclusions on this basis alone.

Conclusions

The results of this work show that substituted catechols are oxidized to their respective quinones. The quinone is then attacked by the various anionic forms of the catechol to form a diphenyl ether. The overall oxidation is a two-electron process, but the coulometric n-value increases at long electrolysis times due to some slowly formed polymeric products and also changes in the reaction mechanism due to the depletion of catechol. Finally, the Hammett ρ-σ plot is consistent with a substantial negative charge in the transition state.

Acknowledgment

The authors would like to acknowledge the Research Corporation and the Marquette University Committee on Research for partial support of this research. In addition, the authors would like to thank the Computer Services Division of Marquette University for computer time, Dennis H. Evans for his generous help in allowing the use of some of his equipment, and Benjamin A. Feinberg for obtaining the mass spectra.

Manuscript submitted Sept. 28, 1979; revised manuscript received Feb. 14, 1980. This was Paper 321 presented at the Boston, Massachusetts, Meeting of the Society, May 6-11, 1979.

Any discussion of this paper will appear in a Discussion Section to be published in the June 1981 JOURNAL. All discussions for the June 1981 Discussion Section should be submitted by Feb. 1, 1981.

REFERENCES

1. R. N. Adams, M. D. Hawley, and S. W. Feldberg, *J. Chem. Phys.*, **71**, 851 (1967).
2. M. D. Hawley, S. V. Tatawawadi, S. Piekarski, and R. N. Adams, *J. Am. Chem. Soc.*, **89**, 447 (1967).
3. A. W. Sternson, R. McCreery, B. Feinberg, and R. N. Adams, *J. Electroanal. Chem. Interfacial Electrochem.*, **46**, 313 (1973).
4. L. Papouchado, G. Petrie, and R. N. Adams, *ibid.*, **38**, 389 (1972).
5. L. Papouchado, G. Petrie, J. H. Sharp, and R. N. Adams, *J. Am. Chem. Soc.*, **90**, 5620 (1968).
6. T. E. Young, J. R. Griswold, and M. H. Hulbert, *J. Org. Chem.*, **39**, 1980 (1974).
7. A. Brun and R. Rosset, *J. Electroanal. Chem. Interfacial Electrochem.*, **49**, 287 (1974).
8. J. Doskocil, *Coll. Czech. Chem. Commun.*, **15**, 780 (1950).
9. G. Sivaramiah and V. R. Krishman, *Indian J. Chem.*, **4**, 541 (1966).
10. D. I. Stom and S. N. Suslov, *Biofizika*, **21**, 40 (1976).
11. H. Musso, in "Oxidative Coupling of Phenols," W. I. Taylor and A. R. Battersley, Editors, pp. 1-94, Marcel Dekker, Inc., New York (1967).
12. W. G. C. Forsyth and V. C. Quesnel, *Biochim. Biophys. Acta.*, **25**, 155 (1957).
13. A. C. Waiss, Jr., J. A. Kuhnle, J. J. Windle, and A. K. Wiersema, *Tetrahedron Lett.*, 6251 (1966).
14. D. E. Hathway, *J. Chem. Soc.*, 519 (1957).
15. C. R. Dawson and W. B. Tarpley, *N.Y. Acad. Sci. Ann.*, **100**, 937 (1963).
16. P. J. Kinlen, D. H. Evans, and S. F. Nelsen, *J. Electroanal. Chem. Interfacial Electrochem.*, **97**, 265 (1979).
17. E. Ritchie, *J. Proc. R. Soc. N.S. Wales*, **78**, 134 (1945).
18. J. F. W. McOmie, M. L. Watts, and D. E. West, *Tetrahedron*, **24**, 2289 (1968).
19. S. W. Feldberg, in "Electroanalytical Chemistry," Vol. 3, A. J. Bard, Editor, pp. 199-296, Marcel Dekker, Inc., New York (1969).
20. P. J. Antikainen and U. Witikainen, *Acta Chem. Scand.*, **27**, 2075 (1973).